Susceptibility of the QCD vacuum to CP-odd electromagnetic background fields

Massimo D'Elia
*Dipartimento di Fisica dell'Università di Pisa and INFN - Sezione di Pisa, Largo Pontecorvo 3, I-56127 Pisa, Italy**

Marco Mariti
Dipartimento di Fisica dell'Università di Pisa, Largo Pontecorvo 3, I-56127 Pisa, Italy†

Francesco Negro
Dipartimento di Fisica dell'Università di Genova and INFN - Sezione di Genova, Via Dodecaneso 33, I-16146 Genova, Italy‡

(Dated: September 5, 2012)

We investigate two flavor QCD in presence of CP-odd electromagnetic background fields and determine, by means of lattice QCD simulations, the induced effective θ term to the first order in $\vec{E} \cdot \vec{B}$. We employ a rooted staggered discretization and study lattice spacings down to 0.1 fm, with pion masses around 400 MeV. In order to deal with a positive measure, we consider purely imaginary electric fields and real magnetic fields, then exploiting analytic continuation. Our results are relevant to a description of the effective pseudoscalar QED-QCD interactions.

PACS numbers: 12.38.Aw, 11.15.Ha,12.38.Gc

I. INTRODUCTION

Quantum ChromoDynamics (QCD) may contain interactions which violate CP, the symmetry under charge conjugation and parity, corresponding to a term $-i\,\theta\, Q$ in the Euclidean action, where

$$Q = \int d^4x\, q(x) = \int d^4x \frac{g^2}{64\pi^2} G^a_{\mu\nu}(x) \tilde{G}^a_{\mu\nu}(x) \qquad (1)$$

is the topological charge operator, $G^a_{\mu\nu}$ is the non-Abelian gauge field strength and $\tilde{G}^a_{\mu\nu} = \epsilon_{\mu\nu\rho\sigma} G^a_{\rho\sigma}$. However, experimental upper bounds on the parameter θ are quite stringent, $|\theta| \lesssim 10^{-10}$ [1, 2]. Nevertheless, θ related effects play an important role in strong interaction phenomenology and are generally linked to fluctuations of Q, which affect, through the axial anomaly, the balance of chirality.

A significant interest has been raised recently by the possibility that local effective variations of θ, corresponding to topological charge fluctuations, may induce detectable phenomena in presence of magnetic fields as strong as those produced in the early phases of non-central heavy ion collisions, which can reach up to 10^{15} Tesla at LHC. According to the so-called chiral magnetic effect [3–5], the net unbalance of chirality induced by the topological background would lead, in presence of a magnetic field strong enough to align the magnetic moments of quarks, to a net separation of electric charge along the field direction.

The physics of strong interactions in presence of electromagnetic (e.m.) backgrounds has attracted much interest also in relation to the possible effects of the background field on the QCD vacuum and on the QCD phase diagram, stimulating a number of model computations and, more recently, of lattice simulations. Such effects may be relevant in various contexts: magnetic fields of the order of 10^{16} Tesla may have been produced at the cosmological electroweak phase transition [6]; large magnetic fields are also expected in compact astrophysical objects such as magnetars [7].

One aspect, emerging from recent lattice simulations with dynamical fermions [8–13] and from model studies [14–16], is that e.m. background fields, even if directly coupled only to charged particles, may have a significant influence, via quark loop effects, also on the gluonic sector. In this study, in an attempt to better clarify such issue, we will investigate how the explicit breaking of some symmetry by the e.m. background field propagates to gluon fields, considering the particular case of CP symmetry.

To be more specific, let us consider QCD in presence of a constant and uniform e.m. field such that $F_{\mu\nu}\tilde{F}_{\mu\nu} \propto \vec{E} \cdot \vec{B} \neq 0$: such background is expected to induce an effective CP-violating interaction in the gluon sector, $\theta_{\rm eff} \frac{g^2}{64\pi^2} G^a_{\mu\nu}(x)\tilde{G}^a_{\mu\nu}(x)$. $\theta_{\rm eff}$ must be an odd function of $\vec{E} \cdot \vec{B}$ and, at the lowest order, we can write

$$\theta_{\rm eff} \simeq \chi_{CP}\, e^2 \vec{E} \cdot \vec{B} + O((\vec{E} \cdot \vec{B})^3) \qquad (2)$$

where χ_{CP} is a sort of susceptibility of the QCD vacuum to CP-breaking e.m. fields.

The effect that we want to study is in some sense complementary to the chiral magnetic effect, where a CP-violating non-Abelian background gives rise to charge separation, hence to an electric field, parallel to a back-

*Electronic address: delia@df.unipi.it
†Electronic address: marco.mariti@gmail.com
‡Electronic address: fnegro@ge.infn.it

ground magnetic field: in that case CP violation propagates from the gluonic to the e.m. sector, i.e. opposite to what we investigate here. In fact, χ_{CP} is directly related to the strength of the effective pseudoscalar QED-QCD interaction, $\chi_{CP}\, q(x)\, e^2\, \vec{E}\cdot\vec{B}$ [17–19]; in particular, to connect with the notation of Ref. [19], we have $\chi_{CP} = \kappa/2$, with κ defined as in Eq. (5) of Ref. [19].

The purpose of this study is to furnish a first determination of χ_{CP} based on lattice QCD simulations. To that aim we will do simulations of QCD in presence of uniform e.m. background fields such that $\vec{E}\cdot\vec{B} \neq 0$, and then we will determine the corresponding induced $\theta_{\rm eff}$ by studying the topological charge distribution.

II. THE METHOD

An e.m. background field enters the QCD lagrangean by modifying the covariant derivative of quarks, $D_\mu = \partial_\mu + i\, g A_\mu^a T^a + i\, q A_\mu$, where A_μ is the e.m. gauge potential and q is the quark electric charge. In the simplest discretization on a cubic lattice, that is implemented by adding proper $U(1)$ phases $u_\mu(n)$ to the usual $SU(3)$ parallel transports, $U_\mu(n) \to u_\mu(n) U_\mu(n)$, where n is a lattice site.

A constant and uniform e.m. field with a single non vanishing component $F_{\mu\nu} = F$ can be realized by a potential $A_\nu = F x_\mu$ and $A_\rho = 0$ for $\rho \neq \nu$. In presence of periodic boundary conditions (b.c.), which is the usual choice in lattice simulations to minimize finite size effects, F must be integer multiple of a minimum quantum

$$f = 2\pi/(q a^2 L_\mu L_\nu)\,, \tag{3}$$

and proper b.c. must be chosen for fermions, to preserve gauge invariance [20]. The corresponding $U(1)$ lattice links are

$$u_\nu^{(q)}(n) = e^{i\, a^2 q F\, n_\mu} \quad ; \quad u_\mu^{(q)}(n)|_{n_\mu = L_\mu} = e^{-i\, a^2 q L_\mu F\, n_\nu} \tag{4}$$

and $u_\rho(n) = 1$ otherwise, where L_μ is the number of lattice sites in the μ direction. In presence of various non-vanishing components of $F_{\mu\nu}$, the definition above generalizes by simply writing the phase of each $U(1)$ link as the sum of the contributions from the various non-vanishing components of $F_{\mu\nu}$.

In the following we shall consider two flavor QCD with fermions discretized in the standard rooted staggered formulation. In the corresponding functional integral, each quark is described by the fourth root of the fermion matrix determinant:

$$Z \equiv \int \mathcal{D}U e^{-S_G} \det M^{\frac{1}{4}}[U, q_u] \det M^{\frac{1}{4}}[U, q_d] \tag{5}$$

$$\begin{aligned} M_{i,j} = am\delta_{i,j} \;+\; \frac{1}{2}\sum_{\nu=1}^{4} \eta_\nu(i) \Big(& u_\nu^{(q)}(i)\; U_\nu(i) \delta_{i,j-\hat\nu} \\ & -\; u_\nu^{*(q)}(i-\hat\nu)\; U_\nu^\dagger(i-\hat\nu) \delta_{i,j+\hat\nu} \Big)\,. \end{aligned} \tag{6}$$

$\mathcal{D}U$ is the functional integration over the non-Abelian gauge link variables, S_G is the plaquette action, i and j refer to lattice sites and $\eta_\nu(i)$ are the staggered phases. The choice for the quark charges is standard, $q_u = 2|e|/3$ and $q_d = -|e|/3$, leading to a quantization in units of $f = 6\pi/(|e| a^2 L_\mu L_\nu)$ for each component of $F_{\mu\nu}$.

The addition of pure $U(1)$ phases to the standard $SU(3)$ link variables leaves the spectrum of $M - m\,\mathrm{Id}$ purely imaginary and symmetric under conjugation: that guarantees $\det M > 0$, hence the feasibility of numerical simulations. However, it is easy to realize that $F_{0i} \neq 0$, as defined above, corresponds, when continued to Minkovski space, to a purely imaginary electric field [21, 22].

In order to have a real electric field, one should introduce imaginary components for the gauge potential in Euclidean space, but that would take the u_μ variables out of the $U(1)$ group and make the quark determinant complex, thus introducing a sign problem which hinders numerical simulations. On the other hand, this is expected in view of the phenomenon that we want to explore since, as it is well known, also the formulation of QCD at real non-vanishing θ suffers from a sign problem.

The usual attitude, taken e.g. in lattice studies of the electric polarizabilities of hadrons, is to keep the electric background field purely imaginary, to avoid the sign problem, then exploiting analytic continuation. We shall follow the same approach, making use, in Euclidean space, of the same definition for all components of $F_{\mu\nu}$: that will correspond to real magnetic fields $\vec{B}$ and imaginary electric fields $\vec{E} = i\,\vec{E}_I$. As a consequence, we expect to produce a purely imaginary effective parameter $\theta_{\rm eff} = i\,\theta_{I{\rm eff}}$. On the other hand, working with an imaginary θ is also one of the possible approaches to the study of θ-dependence in QCD [23–27].

The presence of an imaginary θ_I adds a factor $\exp(\theta_I Q)$ to the probability distribution of gauge fields. That will shift the distribution of the topological charge by an amount which, at the linear order in θ_I, is governed by the topological susceptibility χ at $\theta_I = 0$:

$$\langle Q \rangle_{\theta_I} \simeq V\,\chi\,\theta_I = \langle Q^2 \rangle_{\theta=0}\,\theta_I \tag{7}$$

where V is the spacetime volume. That gives us the opportunity of determining the effective $\theta_{I{\rm eff}}$ produced by a given e.m. field as

$$\theta_{I{\rm eff}} \simeq \frac{\langle Q\rangle(\vec{E}_I, \vec{B})}{\langle Q^2\rangle_0} + O((\vec{E}_I\cdot\vec{B})^3) \tag{8}$$

where by $\langle\cdot\rangle_0$ we mean the average taken at zero e.m. field. Corrections to Eq. (8) will be negligible at least in the region of small $\theta_{I{\rm eff}}$ which is relevant to Eq. (2). In the following we will show that the so defined $\theta_{I{\rm eff}}$ is indeed an odd function of $\vec{E}_I\cdot\vec{B}$ alone and, assuming that the theory is analytic at least for small enough background fields, we shall determine the susceptibility χ_{CP} defined in Eq. (2) from the small field behavior of $\theta_{I{\rm eff}}$.

For the determination of Q on gauge configurations,

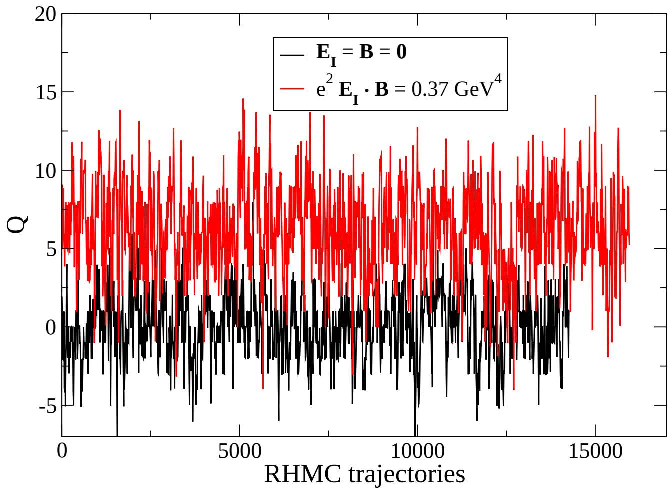

FIG. 1: Monte-Carlo history of Q for $m_\pi \simeq 480$ MeV and $a \simeq 0.12$ fm, on a 16^4 lattice, for two different e.m. backgrounds.

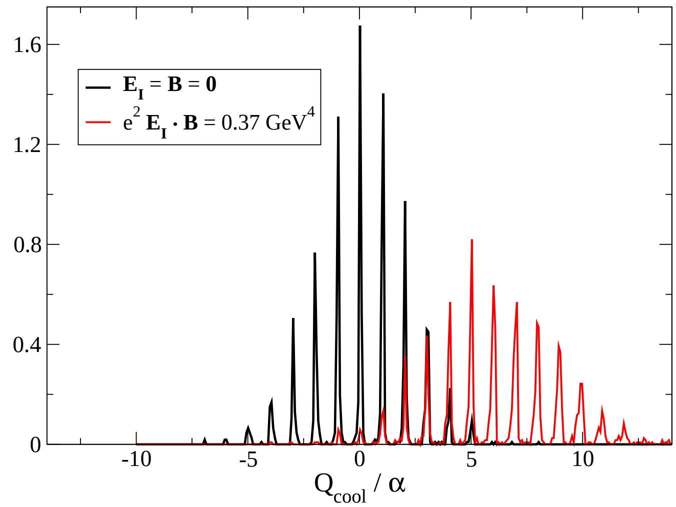

FIG. 2: Distribution of the topological charge after 30 cooling steps. Data are the same as for Fig. 1. The factor α (see text) is 0.947 in this case.

we shall adopt a standard discretized gluonic definition,

$$q_L(x) = \frac{-1}{2^9\pi^2} \sum_{\mu\nu\rho\sigma=\pm 1}^{\pm 4} \tilde{\epsilon}_{\mu\nu\rho\sigma} \mathrm{Tr}\left(\Pi_{\mu\nu}(x)\Pi_{\rho\sigma}(x)\right) \ , \quad (9)$$

measured after cooling [28, 29], i.e. minimization of the pure gauge action to eliminate ultraviolet (UV) artifacts; here $\tilde{\epsilon}_{\mu\nu\rho\sigma} = \epsilon_{\mu\nu\rho\sigma}$ for positive directions and $\tilde{\epsilon}_{\mu\nu\rho\sigma} = -\tilde{\epsilon}_{(-\mu)\nu\rho\sigma}$. Such method is based on the assumption that a given configuration remains in the starting topological sector as the action is minimized; it is known to provide correct results, comparable with improved fermionic definition, as the continuum limit is approached, while maintaining a limited computational cost.

III. RESULTS

We have studied $N_f = 2$ QCD at $T = 0$ (see Eq. (5)), for a fixed pseudo-Goldstone pion mass $m_\pi \simeq 480$ MeV. Different lattice spacings have been explored by tuning the inverse gauge coupling β and am according to what reported in Ref. [30]: $a \simeq 0.30$ fm ($\beta = 5.35, am = 0.075$), $a \simeq 0.20$ fm ($\beta = 5.453, am = 0.02627$), $a \simeq 0.15$ fm ($\beta = 5.527, am = 0.0146$), $a \simeq 0.12$ fm ($\beta = 5.5829, am = 0.01048$) and $a \simeq 0.10$ fm ($\beta = 5.6286, am = 0.008318$). Different lattice volumes have been explored to check for finite size corrections (see Fig. 4).

Numerical simulations have been performed by a standard Rational Hybrid Monte-Carlo (RHMC) algorithm on GPU cards, making use of the code illustrated in Ref. [31]. Typical statistics have been of the order of 10K molecular dynamics time units for each run. The number of (straight) cooling sweeps $n_{\rm cool}$ has varied from 30 for the smallest to 60 for the largest spacing adopted, and it has been chosen in a window where results show no significant dependence on $n_{\rm cool}$. After cooling, the charge is first divided by a constant factor α close to one, so that its distribution gets peaked around integer values (see e.g. Fig. 2), then it is approximated to the closest integer to finally get Q. Autocorrelation times for Q, which are known to grow critically when approaching the continuum limit, have reached up to $O(100)$ RHMC trajectories for $a \simeq 0.1$ fm.

As a first illustration of our results, in Fig. 1 we show the Monte-Carlo history of Q for two numerical simulations performed respectively at zero and non-zero e.m. background field, on a 16^4 lattice with $a \simeq 0.12$ fm and $m_\pi \simeq 480$ MeV. The non-zero e.m. field corresponds to $\vec{E}_I = \vec{B} = 3\, f\, \hat{z}$, where f is defined in Eq. (3), corresponding to $e^2 \vec{E}_I \cdot \vec{B} \simeq 0.37\,\mathrm{GeV}^4$. We see that, while in absence of the e.m. background Q fluctuates around zero, as expected by CP-invariance, fluctuations are shifted towards positive values as $\vec{E}_I \cdot \vec{B} \neq 0$. This is more clearly visible in Fig. 2, where we plot the corresponding distributions of Q; in this particular case we obtain $\langle Q\rangle(\vec{E}_I, \vec{B})/\langle Q^2\rangle_0 = 1.46(14)$.

In order to better investigate the dependence of $\langle Q\rangle(\vec{E}_I, \vec{B})$ on the background field values, in Fig. 3 we show $\langle Q\rangle(\vec{E}_I, \vec{B})/\langle Q^2\rangle_0$ for a 16^4 lattice with $a \simeq 0.3$ fm and $m_\pi \simeq 480$ MeV. Data are obtained for a variety of combinations of $\vec{E}_I$ and $\vec{B}$, mostly taken parallel to the z axis, and then plotted versus $\vec{E}_I \cdot \vec{B}$. The fact that all data fall on the same curve, even when $\vec{E}_I$ and $\vec{B}$ are not parallel, is a nice demonstration that, within errors, $\theta_{I\rm eff}$ is indeed a function of $\vec{E}_I \cdot \vec{B}$ alone, as expected; we have verified that explicitly by taking different combinations of the fields having exactly the same or opposite values for $\vec{E}_I \cdot \vec{B}$, thus checking also that $\theta_{I\rm eff}$ is odd in $\vec{E}_I \cdot \vec{B}$. The dependence is linear in $\vec{E}_I \cdot \vec{B}$ for small fields, then

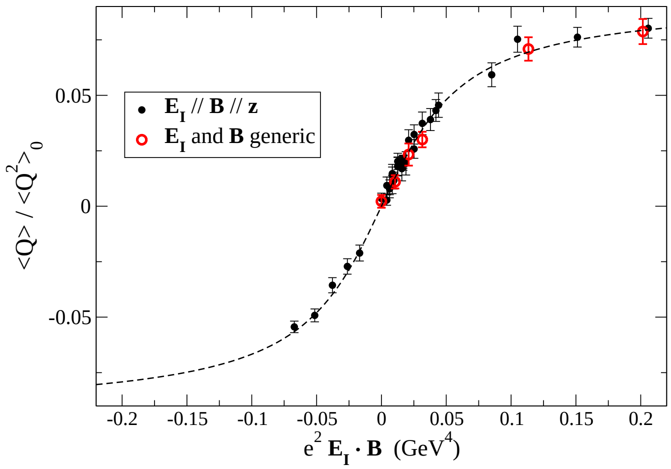

FIG. 3: $\langle Q\rangle(\vec{E}_I, \vec{B})/\langle Q^2\rangle_0$ for various $(\vec{E}_I, \vec{B})$ on a 16^4 lattice for $m_\pi \simeq 480$ MeV and $a \simeq 0.3$ fm. Open circles corresponds to the following combinations of $\vec{E}_I \cdot \vec{B}/f^2$: $(2, -8, -2) \cdot (8, 1, 4)$, $(1, 2, 3) \cdot (3, 2, 1)$, $(1, 3, 4) \cdot (2, 2, 3)$, $(5, 5, 5) \cdot (1, 2, 3)$, $(6, 6, 6) \cdot (6, 6, 6)$, and $(8, 8, 8) \cdot (8, 8, 8)$. The dashed line corresponds to a best fit to Eq. (10).

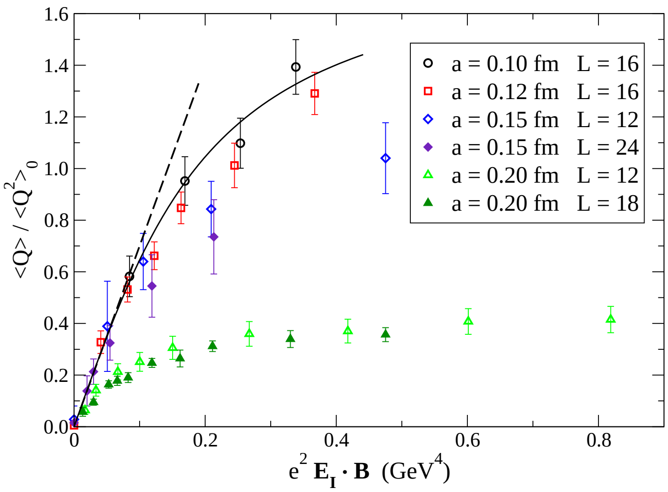

FIG. 4: $\langle Q\rangle(\vec{E}_I, \vec{B})/\langle Q^2\rangle_0$ as a function of $\vec{E}_I \cdot \vec{B}$ for $m_\pi \simeq 480$ MeV and different spacings a and lattice volumes L^4. The continuous line corresponds to a best fit to Eq. (10) at the smallest value of a, the dashed line is the corresponding slope at $\vec{E}_I \cdot \vec{B} = 0$.

showing signs of saturation for larger fields, as common to many systems with a linear response to external stimulation. We have found that all data can be nicely fitted by a function

$$\langle Q\rangle(\vec{E}_I, \vec{B})/\langle Q^2\rangle_0 = a_0 \text{ atan}(a_1 \vec{E} \cdot \vec{B})\,; \qquad (10)$$

the best fit curve, corresponding to $\chi^2/\text{d.o.f.} = 0.74$, is shown in Fig. 3.

In order to discuss finite size and finite UV cutoff effects, in Fig. 4 we show $\langle Q\rangle(\vec{E}_I, \vec{B})/\langle Q^2\rangle_0$ for $m_\pi \simeq 480$ MeV and different spacings a and lattice volumes L^4. $\langle Q\rangle$ and $\langle Q^2\rangle_0$ are both derivatives of the free energy with respect to θ, hence they are proportional to V and, apart from possible systematic effects, their ratio should be independent of V. From Fig. 4 we infer that finite size effects are not significant, even on the smallest volumes explored, corresponding to $am_\pi L \sim 4$.

The dependence on the UV cutoff instead seems significant until $a \lesssim 0.15$ fm. Apart from standard lattice artifacts related to the path integral discretization, additional systematic effects may be related to the method used to determine Q: if a is so coarse that part of the topological background, created by the influence of the e.m. field, lives close to the UV scale, then cooling is expected to destroy part of such background. However data obtained for $a \lesssim 0.15$ fm are in fairly good agreement with each other, within errors, especially in the small field region, which is the one relevant for the determination of χ_{CP}.

In order to determine χ_{CP}, we have performed best fits of the data in Fig. 4 to the function in Eq. (10), in a range $e^2\vec{E}_I \cdot \vec{B} < 0.6$ GeV^4, then considering its slope at $\vec{E}_I \cdot \vec{B} = 0$ and exploiting Eqs. (2) and (8). We have verified that, for each set, the slope is consistent, within errors, with a direct linear fit restricted to a narrow enough region of small $\vec{E}_I \cdot \vec{B}$. We obtain, for the smallest lattice spacings, $\chi_{CP} = 7.1(6)$ GeV^{-4} for $a = 0.15$ fm, $\chi_{CP} = 6.9(5)$ GeV^{-4} for $a = 0.12$ fm and $\chi_{CP} = 7.2(7)$ GeV^{-4} for $a = 0.10$ fm, so that we can quote $\chi_{CP} = (7 \pm 1)$ GeV^{-4} as a reasonable estimate for this value of the pion mass. Preliminary results obtained on a 16^4 lattice and for $a \simeq 0.15$ fm indicate instead $\chi_{CP} \simeq 10(1)$ GeV^{-4} if $m_\pi \simeq 280$ MeV, suggesting that χ_{CP} tends to increase when approaching the chiral limit.

IV. DISCUSSION

It is useful to compare our results with the phenomenological estimate of $\kappa = 2\,\chi_{CP}$ given in Ref. [19], which is based on the effective couplings of the η and η' mesons to two photons and to two gluons: $\chi_{CP} \approx 0.73/(\pi^2 f_\eta^2 m_{\eta'}^2) \sim 3$ GeV^{-4}: even considering the different systematics (the phenomenological estimate is based on a theory with 2+1 light flavors), our data suggest that the lattice QCD result for the effective pseudoscalar QED-QCD interaction is larger, even if of the same order of magnitude.

Regarding the validity of analytic continuation from imaginary to real electric fields, we notice that, while a smooth behavior is expected as the imaginary electric field approaches zero, at least for non-zero quark masses, a non-zero and constant real electric field, however small, is instead expected to induce vacuum instabilities. On the other hand this is not true in presence of an infrared cutoff, i.e. if electric fields are limited in space. Therefore our result should be applicable to determine the local effective θ parameter produced by smooth enough but

limited in space CP-violating e.m. fields. It would be interesting in the future to consider the case of smoothly varying fields explicitly.

In order to give an idea of the magnitude of the effect that we have studied, our estimate predicts that two parallel magnetic and electric fields, with $eB \sim 1$ GeV^2 and $eE \sim 1$ MeV^2, would induce an effective θ of the order of 10^{-5}.

Finally, apart from repeating our determination with more physical quark masses and closer to the continuum limit, it would be interesting to extend our investigation also to finite temperature, especially across and right above the deconfinement transition, where the determination of the effective pseudoscalar QED-QCD interaction would be relevant also to the phenomenology of the chiral magnetic effect in heavy ion collisions.

Acknowledgments

We thank A. Alexandru, C. Bonati, A. Di Giacomo and E. Vicari for useful discussions. Numerical computations have been performed on computer facilities provided by INFN, in particular on two GPU farms in Pisa and Genoa and on the QUONG GPU cluster in Rome. We thank the Galileo Galilei Institute for Theoretical Physics for the hospitality during the completion of this work.

---

[1] P. G. Harris *et al.*, Phys. Rev. Lett. **82**, 904 (1999).
[2] C. A. Baker *et al.*, Phys. Rev. Lett. **97**, 131801 (2006) [hep-ex/0602020].
[3] A. Vilenkin, Phys. Rev. D **22**, 3080 (1980).
[4] D. E. Kharzeev, L. D. McLerran and H. J. Warringa, Nucl. Phys. A **803**, 227 (2008), [arXiv:0711.0950 [hep-ph]]
[5] K. Fukushima, D. E. Kharzeev and H. J. Warringa, Phys. Rev. D **78**, 074033 (2008), [arXiv:0808.3382 [hep-ph]].
[6] T. Vachaspati, Phys. Lett. B **265**, 258 (1991).
[7] R. C. Duncan and C. Thompson, Astrophys. J. **392**, L9 (1992).
[8] M. D'Elia, S. Mukherjee, F. Sanfilippo, Phys. Rev. D **82**, 051501 (2010) [arXiv:1005.5365 [hep-lat]].
[9] M. D'Elia and F. Negro, Phys. Rev. D **83**, 114028 (2011) [arXiv:1103.2080 [hep-lat]].
[10] G. S. Bali, F. Bruckmann, G. Endrodi, Z. Fodor, S. D. Katz, S. Krieg, A. Schafer and K. K. Szabo, JHEP **1202**, 044 (2012) [arXiv:1111.4956 [hep-lat]].
[11] E. -M. Ilgenfritz, M. Kalinowski, M. Muller-Preussker, B. Petersson and A. Schreiber, Phys. Rev. D **85**, 114504 (2012) [arXiv:1203.3360 [hep-lat]].
[12] G. S. Bali, F. Bruckmann, G. Endrodi, Z. Fodor, S. D. Katz and A. Schafer, arXiv:1206.4205 [hep-lat].
[13] M. D'Elia, arXiv:1209.0374 [hep-lat].
[14] I. A. Shovkovy, arXiv:1207.5081 [hep-ph].
[15] V. A. Miransky and I. A. Shovkovy, Phys. Rev. D **66**, 045006 (2002);
[16] B. V. Galilo and S. N. Nedelko, Phys. Rev. D **84**, 094017 (2011).
[17] H. T. Elze and J. Rafelski, In *Sandansky 1998, Frontier tests of QED and physics of the vacuum* 425-439 [hep-ph/9806389].
[18] H. T. Elze, B. Muller and J. Rafelski, hep-ph/9811372.
[19] M. Asakawa, A. Majumder and B. Muller, Phys. Rev. C **81**, 064912 (2010).
[20] M. H. Al-Hashimi and U. J. Wiese, Annals Phys. **324**, 343 (2009) [arXiv:0807.0630 [quant-ph]]
[21] E. Shintani, S. Aoki, N. Ishizuka, K. Kanaya, Y. Kikukawa, Y. Kuramashi, M. Okawa and A. Ukawa *et al.*, Phys. Rev. D **75**, 034507 (2007) [hep-lat/0611032].
[22] A. Alexandru and F. X. Lee, PoS LATTICE **2008**, 145 (2008) [arXiv:0810.2833 [hep-lat]].
[23] V. Azcoiti, G. Di Carlo, A. Galante and V. Laliena, Phys. Rev. Lett. **89**, 141601 (2002).
[24] B. Alles and A. Papa, Phys. Rev. D **77**, 056008 (2008).
[25] S. Aoki, R. Horsley, T. Izubuchi, Y. Nakamura, D. Pleiter, P. E. L. Rakow, G. Schierholz and J. Zanotti, arXiv:0808.1428 [hep-lat].
[26] H. Panagopoulos and E. Vicari, JHEP **1111**, 119 (2011).
[27] M. D'Elia and F. Negro, Phys. Rev. Lett. **109**, 072001 (2012) [arXiv:1205.0538 [hep-lat]].
[28] B. Berg, Phys. Lett. B **104**, 475 (1981); Y. Iwasaki and T. Yoshie, Phys. Lett. B **131**, 159 (1983); S. Itoh, Y. Iwasaki and T. Yoshie, Phys. Lett. B **147**, 141 (1984); M. Teper, Phys. Lett. B **162**, 357 (1985); E. -M. Ilgenfritz *e al.*, Nucl. Phys. B **268**, 693 (1986); M. Campostrini, A. Di Giacomo, H. Panagopoulos and E. Vicari, Nucl. Phys. B **329**, 683 (1990).
[29] E. Vicari and H. Panagopoulos, Phys. Rept. **470**, 93 (2009).
[30] T. Blum, L. Karkkainen, D. Toussaint and S. A. Gottlieb, Phys. Rev. D **51**, 5153 (1995) [hep-lat/9410014].
[31] C. Bonati, G. Cossu, M. D'Elia and P. Incardona, Comput. Phys. Commun. **183**, 853 (2012) [arXiv:1106.5673 [hep-lat]].